Polarized Time-Resolved Fluorescence Reveals Enzyme-Specific Anisotropy Dynamics of Bound NADPH

Ioanna A. Gorbunova*[1], Denis A. Volkov[2], Maxim E. Sasin[2], Oleg S. Vasyutinskii[2]

[1] Institute for Regenerative Medicine, I.M. Sechenov First Moscow State Medical University, 8 Trubetskay str., Moscow 119991, Russian Federation

[2] Ioffe Institute, Russian Academy of Sciences, 26 Polytekhnicheskaya, Saint Petersburg 194021, Russian Federation

*e-mail: i.gorbunova@mail.ioffe.ru

Abstract. We used time-resolved polarized fluorescence spectroscopy for the study of nicotinamide adenine dinucleotide phosphate (NADPH) bound to isocitrate dehydrogenase (IDH) and alcohol dehydrogenase (ADH). It was shown that the fluorescence lifetimes of bound NADPH are strongly enzyme-dependent and are practically identical to those of bound NADH, indicating that fluorescence lifetime imaging microscopy (FLIM) analysis cannot universally distinguish between these two coenzymes. However, in the polarization-sensitive experiments we observed sub-nanosecond fluorescence anisotropy decay components of NADPH bound to IDH and ADH that we found to be significantly enzyme-specific. This result suggests that combined lifetime and anisotropy analysis provides increased molecular specificity for NAD(P)H.

Keywords: fluorescence anisotropy; NAD(P)H; TCSPC; fluorescence lifetime; laser spectroscopy.

Paper #9501 received 30 Jan 2026; revised manuscript received 28 May 2026; accepted for publication 4 Jun 2026; published online 1 Sep 2026. doi: 10.18287/JBPE26.12.030302.

1 Introduction

Nicotinamide adenine dinucleotide (NAD) and its phosphate form (NADP) play a crucial role in the regulation of cellular metabolic pathways. Their reduced forms, NADH and NADPH, are endogenous fluorophores absorbing in the UV spectral range (330–380 nm) and emitting fluorescence with a maximum near 460 nm. These properties make NAD(P)H an attractive target for non-invasive, label-free optical monitoring of metabolic activity in living cells.

Fluorescence lifetime imaging microscopy (FLIM) of NADH and NADPH is widely used for metabolic imagining cells and tissues. Within FLIM, fluorescence decay curves are recorded pixel by pixel using fast single-photon detectors and a time-correlated single-photon counting system, enabling the determination of distributions of fluorescence lifetimes τ_i and their relative contributions a_i within cells. Fluorescence lifetimes of NAD(P)H have been shown to be highly sensitive to the local molecular environment, binding state, and conformational dynamics, which underlies the application of FLIM for monitoring cellular metabolism [1–12].

As is known [10, 13], free NADH and NADPH have identical spectral and time-resolved photophysical properties, and their combined signal is commonly referred to as NAD(P)H fluorescence. In living cells, NAD(P)H fluorescence decay is typically described by a bi-exponential model with a short lifetime of $\tau_1 \sim 400$ ps, attributed to free NADH, and a longer lifetime of $\tau_2 \sim 1.1$–6.0 ns, associated with enzyme-bound NAD(P)H. Changes in these parameters are widely used to access metabolic shifts, redox balance, and energy production [10, 14–16]. However, NADH and NADPH participate in different metabolic pathways: catabolic and biosynthetic/antioxidant processes, respectively. Since both cofactors exhibit nearly identical photophysical properties in their free form [10, 13], separating the contributions of NADH and NADPH, and therefore distinguishing NADH- and NADPH-dependent metabolic processes by FLIM, remains challenging [2, 4, 6].

Recent studies focused on the fluorescence decay of enzyme-bound NADH and NADPH, suggested that differences between them may be detected. Several studies reported that enzyme-bound NADPH may exhibit longer fluorescence lifetimes than bound

This paper was presented at the International Russian-Chinese Workshop on Light for Life Sciences, St. Petersburg, Russian Federation, October 17 – 20, 2025.

NADH, particularly under conditions of oxidative stress or enhanced NADPH oxidase activity [2, 4, 6, 15, 17, 18]. These observations suggested that fluorescence lifetime could be used to separate bound NADPH from bound NADH. However, more recent works demonstrated that the fluorescence lifetime of enzyme-bound NADH and NADPH strongly depends on a specific enzyme binding site and can vary over a wide range [10, 16]. Moreover, most results on the fluorescence decay of enzyme-bound NADH and NADPH were obtained in living cells without systematic validation in simple solution models, which limits the universality of lifetime-based approaches for separating bound NADH and NADPH. An additional challenge arises from the heterogeneity of NAD(P)H fluorescence decay. Both free and protein-bound NAD(P)H exhibit multiple decay components due to conformational diversity, local mobility, and excited-state interactions [9, 10, 19]. Consequently, simplified mono- or bi-exponential analysis of fluorescence decay in mixtures of free and protein-bound NAD(P)H may lead to a substantial loss of molecular specificity.

It has been suggested that the separation of NADH and NADPH in FLIM can be achieved by means of fluorescence anisotropy measurements. Fluorescence anisotropy provides complementary information on excited-state dynamics and molecular mobility that is not accessible from polarization-insensitive (isotropic) fluorescence decay measurements. In particular, time-resolved anisotropy analysis enables the separation of free and protein-bound NADH based on rotational diffusion times and allows estimation of local coenzyme mobility within enzyme binding sites [1, 3, 10]. Although fluorescence anisotropy of NAD(P)H has already been studied in solutions and enzyme complexes [9, 10, 20], its systematic application to enhance molecular specificity in FLIM remained limited.

In this work, we applied time-resolved polarized fluorescence spectroscopy to study the photophysical properties of NADPH bound to two different enzymes, isocitrate dehydrogenase (IDH) and alcohol dehydrogenase (ADH). It was shown that global analysis of polarized fluorescence decay enables simultaneous determination of fluorescence lifetimes and anisotropy parameters and significantly increases molecular specificity for endogenous NAD(P)H fluorescence. We demonstrated that fluorescence anisotropy decay times τ_{ani} and fundamental anisotropy r_0 of NADPH bound to IDH and ADH differ significantly. These differences reflect distinct NADPH mobility depending on the enzyme binding site and enable improved differentiation of enzyme-bound states. Anisotropic fluorescence decay parameters of NADH and NADPH bound to ADH were compared and clear differences between them were obtained. These results highlight polarization-sensitive measurements as a powerful extension of conventional lifetime analysis for resolving metabolic heterogeneity and separating NADH and NADPH contributions in biological systems.

2 Methods

2.1 Materials

The β-NADH (disodium salt, purity >99%, DIA-M, Russia), β-NADPH (disodium salt, purity >98%, Macklin, lot C804424), malate dehydrogenase from porcine heart (>600 units/mg protein, biuret method, ammonium sulfate suspension, lot M1567, Sigma-Aldrich), isocitrate dehydrogenase from porcine heart (Type IV, buffered aqueous glycerol solution, 3–20 units/mg protein, lot I2002, Sigma-Aldrich), and alcohol dehydrogenase (lyophilized powder, recombinant from *E. coli*, 5.0–15.0 U/mg, lot 49854, Sigma-Aldrich) were used in this study. The free NADPH was dissolved in buffer solution in the concentration of 60 μM and then IDH or ADH was added to the solution. The IDH and ADH concentration was at about 130 μM. All solutions were prepared in phosphate buffer (PBS) at pH = 7.2. The units U/mg and U/mL denote enzyme activity normalized to the mass or volume of the reagent, respectively. Here, "U" refers to enzyme units, which represent the amount of active enzyme required to catalyze a defined reaction under specified conditions.

2.2 Experimental Procedure

The procedure for experimental detection of polarized fluorescence decay signals was the same as described in our previous publication [8]. The molecular fluorescence was two- photon excited at 720 nm with a femtosecond Ti : sapphire laser (Mai Tai HP, Spectra Physics, USA). The pulse duration was of 100 fs and a repetition rate of 80 MHz. The average laser power at the molecular sample position was 500 mW.

Polarized fluorescence was collected in a direction perpendicular to the excitation beam propagation and detected in the range of 440–480 nm. Two orthogonal polarization components of fluorescence, parallel ($I_{\parallel}$) and perpendicular ($I_{\perp}$) to the polarization excitation beam, were separated using a Glan prism. The two polarization components were then detected simultaneously and independently by two ultrafast avalanche photodiodes (APD-050-CTC, MPD, Germany) operating in the photon-counting mode. The detected signals were processed using a time-correlated single-photon counting (TCSPC) system (PicoHarp 300, PicoQuant, Germany) with a time resolution of 4 ps per channel. The instrumental response function IRF(t) was determined experimentally by detecting scattered laser radiation at wavelengths corresponding to the fluorescence detection range of NADPH.

2.3 Experimental Signal Processing

For analysis of the orthogonally polarized fluorescence signals of NADPH-IDH and NADPH-ADH complexes in solution the following model was used [9]:

$$I_{\parallel}(t) = G\sum_k \left[I_{iso}^k(t)\left(1 + 2r^k(t)\right)\right] * \mathrm{IRF}(t) + y, \quad (1)$$

$$I_{\perp}(t) = \sum_k \left[I_{iso}^k(t) \left(1 - r^k(t)\right)\right] * \mathrm{IRF}(t) + y, \quad (2)$$

where $I_{iso}^k(t)$ is the isotropic (polarization-insensitive) fluorescence decay, $r^k(t)$ is the fluorescence anisotropy decay, y is a background, and $\mathrm{IRF}(t)$ is the instrumental response function. The factor $G = I_Y/I_X$, where I_Y and I_X are the fluorescence components polarized along the Y and X directions, respectively, with both components being orthogonal to the excitation light, accounts for differences in the polarization sensitivity of the two detection channels. The index k denotes f and b, which correspond to free and enzyme-bound NADPH, respectively. This model allows the determination of isotropic fluorescence decay $I_{iso}(t)$ and anisotropy decay $r(t)$ parameters for free and bound species.

The isotropic fluorescence decay of free and enzyme-bound NADPH exhibited heterogeneous behavior and was described by a sum of exponents:

$$I_{iso}^{f/b}(t) = I_0^{f/b} \sum_{i=1}^{n} a_i \exp\left(-\frac{t}{\tau_i}\right), \quad (3)$$

where $I_0^{f/b}$ is the fluorescence intensity contribution of the corresponding species at $t = 0$, τ_i are fluorescence decay times, and a_i are their weighting coefficients.

The fluorescence anisotropy decay of free NADPH was described by a single-exponential function:

$$r^f(t) = r_0 \exp\left(-\frac{t}{\tau_r}\right), \quad (4)$$

where r_0 is the anisotropy and τ_r is the rotational diffusion time.

In the case of coenzyme-enzyme complexes we took into consideration of different possible depolarization processes in coenzyme excited state and used the expression suggested in our recent publication [19]:

$$r^b(t) = \left(r_{b1} + r_{b2} e^{-t/\tau_{bv}}\right) e^{-t/\tau_{br}}, \quad (5)$$

where τ_{bv} characterizes fast depolarization associated with anisotropic vibrational relaxation and τ_{br} characterizes the rotational diffusion time of the entire complex.

3 Results

The fluorescence decay signals of the orthogonal components of polarized fluorescence for IDH and ADH solutions with the addition of 60 μ M free NADPH, obtained under two-photon excitation at 733 nm, are shown in Fig. 1(b) and (c), respectively. For comparison, Fig. 1(a) presents the polarized fluorescence decay signals of free NADPH in PBS.

To perform global fitting of the polarized fluorescence decay signals of NADPH in the presence of IDH and ADH, a model accounting for contributions from free NADPH and enzyme-bound NADPH was used. The fluorescence decay parameters of free NADPH were determined independently from the analysis of the signals shown in Fig. 1(a) and were fixed during the fitting procedure. Using this approach, the fluorescence decay parameters of the NADPH-IDH and NADPH-ADH complexes were extracted and are summarized in Tables 1 and 2, respectively.

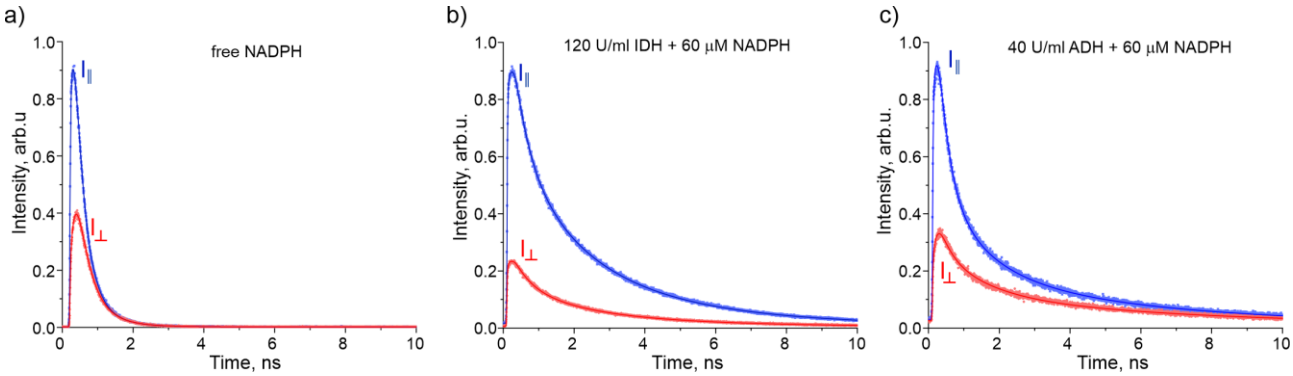

Fig. 1 Orthogonally polarized fluorescence decay signals corresponding to the components parallel ($I_{\parallel}$, blue curve) and perpendicular ($I_{\perp}$, red curve) to the excitation light polarization: (a) free NADPH, (b) solution of 120 U/ml IDH and 60 μM NADPH, and (c) solution of 40 U/ml ADH and 60 μM NADPH. U/mL denotes enzyme activity normalized to the solution volume.

Table 1 Polarized fluorescence decay parameters in NADPH bound with IDH determined by the global fit.

λ_{ex}, nm	τ_{b1}, ns (a_1)	τ_{b2}, ns (a_2)	r_{b1}	r_{b2}	τ_{bv}, ns	τ_r, ns
733	2.27 (0.83)	5.67 (0.17)	0.52	0.02	0.67	50
750	2.28 (0.83)	5.70 (0.17)	0.51	0.02	1.01	50
770	2.26 (0.79)	5.60 (0.21)	0.50	0.06	0.90	50
Uncertainty	±0.25 (±0.07)	±0.30 (±0.07)	±0.02	±0.02	±0.07	–

Table 2 Polarized fluorescence decay parameters in NADPH bound with ADH determined by the global fit.

λ_{ex}, nm	τ_{b1}, ns	r_{b1}	r_{b2}	τ_{bv}, ns	τ_r, ns
733	5.31	0.21	0.22	0.36	10
750	4.90	0.23	0.23	0.24	10
770	5.07	0.23	0.24	0.26	10
Uncertainty	±0.30	±0.02	±0.02	±0.07	–

It was found that the NADPH-IDH complex exhibits a bi-exponential fluorescence decay with decay times of $\tau_1 \approx 2.3$ ns ($a_1 = 0.83$) and $\tau_2 \approx 5.7$ ns ($a_2 = 0.17$). In contrast, the NADPH-ADH complex is characterized by a single dominant fluorescence decay component with $\tau_1 \approx 5.0$ ns. The obtained decay times and their relative contributions were practically independent of the excitation wavelength. Notably, the fluorescence decay times of NADPH bound to IDH and ADH were significantly longer than those of free NADPH in solution. In addition, free NADPH exhibited biexponential fluorescence decay, whereas only a single decay component was observed for the NADPH-ADH complex.

Global fitting of the experimental data in Fig. 1 was further used to analyze the fluorescence anisotropy decay of NADPH-enzyme complexes. The anisotropy decay was described using a model previously developed for coenzyme-enzyme complexes, which allows separation of multiple anisotropic relaxation processes associated with different types of dipole reorientation. These processes include rotational diffusion of the entire complex, local mobility of the coenzyme within the enzyme binding site, reorientation due to nuclear rearrangement during excited-state vibrational relaxation, and resonant energy transfer (FRET) between chromophores located at different binding sites within dimeric enzymes. The fluorescence anisotropy decay parameters obtained from global fitting are summarized in Tables 1 and 2 for the NADPH-IDH and NADPH-ADH complexes, respectively.

As follows from the obtained parameters, the fluorescence anisotropy decay of enzyme-bound NADPH is characterized by two depolarization times. A short depolarization time τ_{bv} of approximately 0.3 ns and 1.0 ns was observed for the NADPH-ADH and NADPH-IDH complexes, respectively, while long rotational diffusion times τ_{br} of approximately 20 ns and 100 ns were determined for the NADPH-ADH and NADPH-IDH complexes, respectively. Significant differences were also observed in the corresponding anisotropy amplitudes r_{b1} and r_{b2}.

For the NADPH-IDH complex, the anisotropy amplitude r_{b1} was 0.52, close to the fundamental anisotropy of free NADPH $r_0 \approx 0.5$, whereas the amplitude r_{b2} associated with the short depolarization component was very small (0.02). In contrast, for the NADPH-ADH complex, r_{b1} was 0.22, more than two times lower than that of free NADPH and the NADPH-IDH complex. At the same time, the anisotropy amplitude r_{b2} for the NADPH-ADH complex was significantly larger (0.23) than that for the NADPH-IDH complex.

It is noteworthy that the anisotropy amplitude $r_{b2} \approx 0.23$ for the NADPH-ADH complex coincides with the corresponding parameter previously reported for the NADH-ADH complex. However, the short depolarization time $\tau_{bv} \approx 0.3$ ns observed for NADPH-ADH is considerably shorter than that reported earlier for NADH-ADH ($\tau_{bv} \sim 1$ ns).

4 Discussion

4.1 Fluorescence Lifetimes of Bound NADH and NADPH

One of the central challenges in NAD(P)H-FLIM is the separation of NADH and NADPH fluorescence signals in cells. Because free NADH and NADPH have identical fluorescence spectra and fluorescence lifetimes, they cannot be distinguished in the free form. For this reason, recent studies [9, 10] have focused on enzyme-bound cofactors and suggested that differences in fluorescence decay times of bound NADH and NADPH may enable their separation. In particular, Blacker et al. reported that the NADPH-NOX complex exhibits a significantly longer fluorescence lifetime than bound NADH and proposed a general rule that enzyme-bound NADPH has a longer fluorescence decay time than NADH, independent of the enzyme. However, studies of NAD(P)H-enzyme complexes in solution demonstrate that fluorescence decay times of NADH and NADPH strongly depend on the specific enzyme binding site. Table 3 summarizes representative fluorescence decay parameters reported for various NADH- and NADPH-dependent dehydrogenases. As can be seen in Table 3, both the absolute decay times and the number of decay components vary significantly between enzymes. In several cases, bound NADH exhibits fluorescence decay times comparable to or even longer than those of bound NADPH, indicating that a simple lifetime-based distinction between NADH and NADPH is not universal. In addition to enzyme specificity, another important factor affecting fluorescence decay analysis is the heterogeneity of free NADH fluorescence.

Table 3 Fluorescence decay times τ_i and weighting coefficients a_i of NAD(P)H-enzyme complexes reported in the literature.

Species	λ_{ex}, λ_{fluo}	τ_1 (ns) (a_1)	τ_2 (ns) (a_2)	Source
NADH-LDH	340 nm, 368–600 nm	1.34 (0.22)	3.20 (0.09)	[10]
	340 nm, 368–600 nm	–	3.34 (0.09)	[21]
	750 nm, 440/40 nm	–	1.60 (1.00)	[14]
NADH-MDH	720 nm, 436/10 nm	–	1.24 (1.00)	[16]
	750 nm, 440/40 nm	–	1.20 (1.00)	[14]
NADH-ADH	720 nm, 436/10 nm	–	4.44 (1.00)	[9]
NADPH-IDH	340 nm, 368–600 nm	1.59 (0.12)	4.44 (0.02)	[10]
	760 nm, 466/30 nm	–	2.20 (1.00)	[16]
NADPH-G6PDH	750 nm, 440/40 nm	–	2.50 (1.00)	[16]

Free NAD(P)H fluorescence decay is heterogeneous and is characterized by two decay components with lifetimes of approximately $\tau_1 \sim 0.25$ ns and $\tau_2 \sim 0.6$ ns, which have been attributed to two distinct cis and trans conformations of the nicotinamide moiety. Approximating the fluorescence decay of free NAD(P)H by a single-exponential function, as was done in several studies listed in Table 3, can lead to quantitative errors in the determination of fluorescence decay times of enzyme-bound NAD(P)H in mixed systems.

In this work, we applied a refined analysis of fluorescence decay in mixtures of free NADPH and NADPH bound to IDH and ADH. In our model, the heterogeneity of free NADPH fluorescence was explicitly taken into account by describing the free coenzyme with a biexponential decay function. This approach allowed us to determine fluorescence decay times of enzyme-bound NADPH with higher accuracy than in previous studies. We found that the NADPH-IDH complex exhibits two nanosecond fluorescence decay components of approximately 2 ns and 5 ns, whereas the NADPH-ADH complex is characterized by a single fluorescence decay time of about 5 ns. The shorter decay component of the NADPH-IDH complex (~ 2 ns) is consistent with the value reported by Leben et al. [16] but differs from that reported by Blacker et al.

Another important result of this study is the determination of the fluorescence decay time of the NADPH-ADH complex, which has not been reported previously. This result enables a direct comparison of fluorescence decay parameters of NADH and NADPH bound to the same enzyme. We show that the fluorescence decay time of NADPH-ADH (~ 5 ns) determined in this work is not significantly longer than that of NADH-ADH (~4.5 ns) reported in our previous study [9].

Overall, the strong enzyme specificity of NADPH fluorescence lifetimes and the nearly identical fluorescence decay times of NADH and NADPH bound to ADH demonstrate that lifetime-based separation of NADH and NADPH cannot rely on a universal fluorescence lifetime criterion.

4.2 Fluorescence Anisotropy Decay in Bound NADH and NADPH

Here, we show that fluorescence anisotropy decay of bound NADPH is heterogeneous and characterized by two distinct depolarization times of approximately 1 ns and longer than 20 ns, as summarized in Tables 1 and 2. The longer depolarization time corresponds to rotational diffusion of the entire coenzyme–enzyme complex. Elucidation of the origin of the short depolarization time was the main focus of this study.

Heterogeneous fluorescence anisotropy decay is a general feature of fluorophore-macromolecule complexes and has been discussed extensively for a wide range of systems, including fluorescent proteins, dye-labeled DNA, and membrane-associated probes. Two major theoretical frameworks have been proposed to describe fluorescence anisotropy heterogeneity. The first comprises diffusion-based models that account for multiple types of rotational motion, including fast local motions of the fluorophore, slower dynamics of protein structural elements, and global tumbling of the entire complex [22, 23]. The second framework is based on a more general formalism using spherical tensors and correlation functions, in which multiple relaxation pathways contributing to anisotropy decay are taken into account [9, 19, 24].

Among diffusion-based approaches, the "wobbling-in-a-cone" model has been widely used to interpret anisotropy decay of NAD(P)H-enzyme complexes [10, 25, 26]. Within this framework, fluorescence depolarization of bound NADH and NADPH arises from a combination of global rotational

diffusion of the enzyme and restricted local motion of the coenzyme within a cone defined by the geometry of the binding site. Using this model, Blacker et al. [10] concluded that NADPH bound to IDH exhibits significantly faster local motion than NADH bound to LDH, consistent with differences in steric constraints and electrostatic interactions in the respective binding sites.

In contrast, the model used in the present study to analyze fluorescence anisotropy decay of bound NADPH (Eq. (5)) is based on a more general formalism that explicitly separates different anisotropic relaxation processes occurring in the excited state of NADPH. This model was first proposed in our recent paper [19] and successfully applied to the NADH-ADH complex [9]. Within this framework, the anisotropy parameters r_{b1} and r_{b2} in Eq. (5) characterize the relative orientation of the excitation and emission transition dipole moments in the relaxed state and during anisotropic vibrational relaxation, respectively. The parameter r_{b2} reflects changes in the orientation of the fluorescence transition dipole moment induced by fast nuclear relaxation in the excited state of the coenzyme. Correspondingly, the fast fluorescence depolarization time τ_{bv} in Eq. (5) reflects the rate of anisotropic relaxation associated with nuclear rearrangements in the excited state.

We suggest that the short depolarization time of approximately 1 ns observed for the NADPH-IDH and NADPH-ADH complexes reflects the rate of nuclear rearrangements of NADPH in the excited state and can be used as a measure of local coenzyme mobility within the enzyme binding site. For the NADPH-IDH complex, the anisotropy amplitude r_{b1} is close to the fundamental anisotropy of free NADPH, while the parameter r_{b2} associated with the fast depolarization component is close to zero. This indicates that the orientation of the excitation and emission transition dipole moments changes only weakly during excited-state vibrational relaxation, suggesting limited local mobility of NADPH in the IDH binding site under our experimental conditions. In contrast, for the NADPH–ADH complex, the parameter r_{b2} is significantly larger ($r_{b2} = 0.3$), indicating a pronounced reorientation of the transition dipole moment during excited-state relaxation and enhanced local mobility of NADPH in the ADH binding site.

These findings reflect fundamental differences in binding-site mobility and conformational dynamics of NADPH in IDH and ADH. NMR and X-ray studies have shown that dehydrogenases undergo large-amplitude conformational changes during catalysis and exhibit varying degrees of binding-site mobility [27, 28]. Our results indicate that NADPH bound to ADH exhibits higher local mobility than NADPH bound to IDH and is also more mobile than NADH bound to ADH.

We further compared anisotropy decay parameters of NADPH and NADH bound to ADH and revealed coenzyme-specific dynamics within the ADH binding site. We found that the fast depolarization time of the NADPH-ADH complex ($\tau_{bv} \sim 0.3$ ns) is considerably shorter than that of the NADH-ADH complex ($\tau_{bv} \sim 1$ ns). At the same time, the anisotropy amplitude r_{b2} associated with the fast component is nearly identical for NADH and NADPH bound to ADH ($r_{b2} \approx 0.23$). This demonstrates that NADPH experiences faster local depolarization dynamics than NADH in the same enzyme environment.

Overall, these results demonstrate that time-resolved fluorescence anisotropy provides a sensitive probe of local coenzyme mobility and binding-site dynamics. When combined with isotropic fluorescence decay analysis, anisotropy measurements enable discrimination between enzyme-bound NAD(P)H states that cannot be resolved by fluorescence lifetime analysis alone, highlighting their potential for improving molecular specificity in FLIM-based metabolic studies.

5 Conclusion

In this work, we performed a comprehensive time-resolved study of fluorescence decay and anisotropy of NADPH bound to isocitrate dehydrogenase (IDH) and alcohol dehydrogenase (ADH). By combining a global fitting procedure of polarized fluorescence decay signals with explicit consideration of the heterogeneous fluorescence decay of free NADPH, we demonstrated enzyme-specific features of polarized fluorescence decay of NADPH. In particular, we found that the fluorescence lifetime of NADPH bound to IDH is approximately two times shorter than that of the NADH-ADH complex, whereas the fluorescence lifetimes of NADH and NADPH bound to ADH are nearly identical. These results confirm that fluorescence lifetime alone cannot be reliably used to separate NADH and NADPH in living cells by FLIM.

The major result of this study is the observation of heterogeneous fluorescence anisotropy decay in NADPH-enzyme complexes. We show that both NADPH-IDH and NADPH-ADH are characterized by a sub-nanosecond fluorescence depolarization component in addition to a long rotational diffusion time of the entire complex exceeding 20 ns. We suggest that the fast depolarization component reflects rapid nuclear rearrangements of NADPH in the excited state and/or local coenzyme mobility within the enzyme binding site. Importantly, the fast depolarization component differs significantly between NADPH-IDH and NADPH-ADH, indicating enzyme-specific local mobility of NADPH. Moreover, comparison of anisotropy decay of NADPH-ADH and NADH-ADH reveals coenzyme-specific anisotropic excited-state dynamics that are not accessible from isotropic fluorescence lifetime analysis.

Overall, our results demonstrate that combined analysis of isotropic fluorescence decay and fluorescence anisotropy provides additional molecular specificity for endogenous NAD(P)H. This approach opens new opportunities for distinguishing enzyme-bound states and lays the groundwork for extending

polarized FLIM toward improved separation of NADH- and NADPH-related metabolic pathways in complex biological systems.

Disclosures

All authors declare that there is no conflict of interest in this paper.

References

1. H. D. Vishwasrao, A. A. Heikal, K. A. Kasischke, and W. W. Webb, "Conformational Dependence of Intracellular NADH on Metabolic State Revealed by Associated Fluorescence Anisotropy," Journal of Biological Chemistry 280 (26), 25119–25126 (2005).
2. R. Niesner, P. Narang, H. Spiecker, V. Andresen, K.-H. Gericke, and M. Gunzer, "Selective Detection of NADPH Oxidase in Polymorphonuclear Cells by Means of NAD(P)H-Based Fluorescence Lifetime Imaging," Journal of Biophysics 2008, 602639 (2008).
3. Q. Yu, A. A. Heikal, "Two-photon autofluorescence dynamics imaging reveals sensitivity of intracellular NADH concentration and conformation to cell physiology at the single-cell level," Journal of Photochemistry and Photobiology B: Biology 95(1), 46–57 (2009).
4. A. A. Mossakowski, J. Pohlan, D. Bremer, R. Lindquist, J. M. Millward, M. Bock, K. Pollok, R. Mothes, L. Viohl, M. Radbruch, J. Gerhard, J. Bellmann-Strobl, J. Behrens, C. Infante-Duarte, A. Mähler, M. Boschmann, J. L. Rinnenthal, M. Füchtemeier, J. Herz, F. C. Pache, M. Bardua, J. Priller, A. E. Hauser, F. Paul, R. Niesner, and H. Radbruch, "Tracking CNS and systemic sources of oxidative stress during the course of chronic neuroinflammation," Acta Neuropathologica 130(6), 799–814 (2015).
5. O. S. Vasyutinskii, A. G. Smolin, C. Oswald, and K. H. Gericke, "Polarized fluorescence in NADH under two-photon excitation with femtosecond laser pulses," Optics and Spectroscopy 122(4), 602–606 (2017).
6. R. Leben, L. Ostendorf, S. Van Koppen, A. Rakhymzhan, A. Hauser, H. Radbruch, and R. Niesner, "Phasor-Based Endogenous NAD(P)H Fluorescence Lifetime Imaging Unravels Specific Enzymatic Activity of Neutrophil Granulocytes Preceding NETosis," International Journal of Molecular Sciences 19(4), 1018 (2018).
7. M. E. Sasin, I. A. Gorbunova, N. O. Bezverkhnii, Y. M. Beltukov, O. S. Vasyutinskii, and J. Rubayo-Soneira, "Polarized Fluorescence in NADH Two-Photon Excited by Femtosecond Laser Pulses in the Wavelength Range of 720–780 nm," Technical Physics Letters 45(7), 672–674 (2019).
8. I. A. Gorbunova, M. E. Sasin, J. Rubayo-Soneira, A. G. Smolin, and O. S. Vasyutinskii, "Two-Photon Excited Fluorescence Dynamics in NADH in Water–Methanol Solutions: The Role of Conformation States," The Journal of Physical Chemistry B 124(47), 10682–10697 (2020).
9. I. A. Gorbunova, M. E. Sasin, D. P. Golyshev, A. A. Semenov, A. G. Smolin, Y. M. Beltukov, and O. S. Vasyutinskii, "Two-Photon Excited Fluorescence Dynamics in Enzyme-Bound NADH: the Heterogeneity of Fluorescence Decay Times and Anisotropic Relaxation," The Journal of Physical Chemistry B 125(34), 9692–9707 (2021).
10. T. S. Blacker, M. R. Duchen, and A. J. Bain, "NAD(P)H binding configurations revealed by time-resolved fluorescence and two-photon absorption," Biophysical Journal 122(7), 1240–1253 (2023).
11. V. I. Shcheslavskiy, M. V. Shirmanova, K. S. Yashin, A. C. Rück, M. C. Skala, and W. Becker, "Fluorescence Lifetime Imaging Techniques—A Review on Principles, Applications and Clinical Relevance," Journal of Biophotonics 18(12), e202400450 (2025).
12. D. L. Pham, A. A. Gillette, J. Riendeau, K. Wiech, E. C. Guzman, R. Datta, and M. C. Skala, "Perspectives on label-free microscopy of heterogeneous and dynamic biological systems," Journal of Biomedical Optics 29(S2), (2024).
13. E. V. Potapova, E. A. Zherebtsov, V. V. Shupletsov, V. V. Dremin, K. Y. Kandurova, A. V. Mamoshin, A. Y. Abramov, and A. V. Dunaev, "Detection of NADH and NADPH levels in vivo identifies shift of glucose metabolism in cancer to energy production," The FEBS Journal 291(12), 2674–2682 (2024).
14. J. T. Sharick, P. F. Favreau, A. A. Gillette, S. M. Sdao, M. J. Merrins, and M. C. Skala, "Protein-bound NAD(P)H Lifetime is Sensitive to Multiple Fates of Glucose Carbon," Scientific Reports 8(1), 5456 (2018).
15. T. S. Blacker, Z. F. Mann, J. E. Gale, M. Ziegler, A. J. Bain, G. Szabadkai, and M. R. Duchen, "Separating NADH and NADPH fluorescence in live cells and tissues using FLIM," Nature Communications 5(1), 3936 (2014).
16. R. Leben, M. Köhler, H. Radbruch, A. E. Hauser, and R. A. Niesner, "Systematic Enzyme Mapping of Cellular Metabolism by Phasor-Analyzed Label-Free NAD(P)H Fluorescence Lifetime Imaging," International Journal of Molecular Sciences 20(22), 5565 (2019).
17. P. Majumder, T. S. Blacker, L. S. Nolan, M. R. Duchen, and J. E. Gale, "Multiphoton NAD(P)H FLIM reveals metabolic changes in individual cell types of the intact cochlea upon sensorineural hearing loss," Scientific Reports 9(1), 18907 (2019).
18. A. Song, N. Zhao, D. C. Hilpert, C. Perry, J. A. Baur, D. C. Wallace, and P. M. Schaefer, "Visualizing subcellular changes in the NAD(H) pool size versus redox state using fluorescence lifetime imaging microscopy of NADH," Communications Biology 7(1), 428 (2024).

19. I. A. Gorbunova, M. E. Sasin, Y. M. Beltukov, A. A. Semenov, and O. S. Vasyutinskii, "Anisotropic relaxation in NADH excited states studied by polarization-modulation pump–probe transient spectroscopy," Physical Chemistry Chemical Physics 22(32), 18155–18168 (2020).
20. S. Cao, H. Li, Y. Liu, M. Wang, M. Zhang, S. Zhang, J. Chen, J. Xu, J. R. Knutson, and L. Brand, "Dehydrogenase Binding Sites Abolish the "Dark" Fraction of NADH: Implication for Metabolic Sensing via FLIM," The Journal of Physical Chemistry B 124(31), 6721–6727 (2020).
21. S. Ranjit, L. Malacrida, M. Stakic, and E. Gratton, "Determination of the metabolic index using the fluorescence lifetime of free and bound nicotinamide adenine dinucleotide using the phasor approach," Journal of Biophotonics 12(11), e201900156 (2019).
22. C. W. Ko, Z. Wei, R. J. Marsh, D. A. Armoogum, N. Nicolaou, A. J. Bain, A. Zhou, and L. Ying, "Probing nanosecond motions of plasminogen activator inhibitor-1 by time-resolved fluorescence anisotropy," Molecular BioSystems 5(9), 1025–1031 (2009).
23. G. F. Schröder, U. Alexiev, and H. Grubmüller, "Simulation of Fluorescence Anisotropy Experiments: Probing Protein Dynamics," Biophysical Journal 89(6), 3757–3770 (2005).
24. A. Szabo, "Theory of fluorescence depolarization in macromolecules and membranes," The Journal of Chemical Physics 81(1), 150–167 (1984).
25. K. Kinosita, A. Ikegami, and S. Kawato, "On the wobbling-in-cone analysis of fluorescence anisotropy decay," Biophysical Journal 37(2), 461–464 (1982).
26. G. Lipari, A. Szabo, "Effect of librational motion on fluorescence depolarization and nuclear magnetic resonance relaxation in macromolecules and membranes," Biophysical Journal 30(3), 489–506 (1980).
27. S. B. Raj, S. Ramaswamy, and B. V. Plapp, "Yeast Alcohol Dehydrogenase Structure and Catalysis," Biochemistry 53(36), 5791–5803 (2014).
28. B. V. Plapp, B. R. Savarimuthu, D. J. Ferraro, J. K. Rubach, E. N. Brown, and S. Ramaswamy, "Horse Liver Alcohol Dehydrogenase: Zinc Coordination and Catalysis," Biochemistry 56(28), 3632–3646 (2017).